Laser Cooling of a Semiconductor by 40 Kelvin: An Optical Refrigerator Based on Cadmium Sulfide Nanoribbons

Jun Zhang, [†,#] *Dehui Li,* [†,#] *Renjie Chen,* [†] *Qihua Xiong* [†,⊥,*]

[†]Division of Physics and Applied Physics, School of Physical and Mathematical Sciences, Nanyang Technological University, Singapore 637371

[⊥]Division of Microelectronics, School of Electrical and Electronic Engineering, Nanyang Technological University, Singapore 639798

[#]These authors contribute to this work equally.

*To whom correspondence should be addressed. Email address: Qihua@ntu.edu.sg.

ABSTRACT

We have demonstrated the first net laser cooling of semiconductors using CdS nanoribbons (or nanobelts) in this work. This net cooling effect is found to be facilitated by resonant high order annihilation of longitudinal optical (LO) phonons due to a strong exciton-LO phonon Fröhlich interactions. Using a pump-probe luminescence thermometry technique to measure the local temperature change, we have achieved as large as 40 K cooling temperature from room temperature pumped by a 514 nm laser while a 532 nm laser pumping led to a cooling of 20 K. At 100 K, only the 532 nm laser pumping can lead to a net cooling of around 15 K. Our work opens new directions to search laser cooling semiconductors and makes it feasible to achieve all solid-state cryocoolers based on semiconductors.

Keywords: Optical refrigeration, Laser cooling of semiconductors, CdS nanobelts, anti-Stokes luminescence

1. INTRODUCTION

The concept of laser cooling of solids or optical refrigeration was proposed by Pringsheim in 1929[1]. The basic principle of optical refrigeration is anti-Stokes luminescence. Photons in the red tail of the absorption spectrum are absorbed followed by anti-Stokes spontaneous emission, *i.e.*, the emitted photons have higher energy (blue-shifted) than the absorbed photons. During the emission process the lattice thermal vibration energy is carried away by the emitted photons resulting in the laser cooling effect. The process is very similar to Doppler cooling of atoms, except that in cooling of atoms, it is the translational kinetic energy being removed[2]; while in solid materials, the energy is largely contained in lattice vibrations, *i.e.*, phonons. To realize the net laser cooling of solids, the material requires having high purity with proper spaced energy levels and a high external quantum efficiency. Due to those special requirements, the materials for the optical refrigeration are limited to only rare-earth (RE) doped crystals or glasses and direct bandgap semiconductors.

Rare-earth doped materials were proposed for laser cooling in the late 1950s, nearly thirty years after Pringsheim's proposal[3]. However, the difficulty of obtaining high purity materials prevented the net laser cooling from being observed in solids for a long time. The first breakthrough of the net laser cooling in solids

Laser Refrigeration of Solids VI, edited by Richard I. Epstein, Denis V. Seletskiy, Mansoor Sheik-Bahae,
Proc. of SPIE Vol. 8638, 863808 · © 2013 SPIE · CCC code: 0277-786X/13/$18
doi: 10.1117/12.2002713

was achieved in ytterbium-doped glass in 1995[4], around 70 years after the concept was established. The first successful laser cooling effect was only ~ 0.3 K. Since then, great effort has been devoted to improve the cooling efficiency and to reach a larger cooling temperature in a variety of the RE doped crystals and glasses[5]. To date, the minimum achievable temperature of ~ 110 K starting from ambient temperature has been realized in a 5% doped Yb: YLF crystal[6], which surpasses the thermoelectric Peltier coolers.

Compared with the atomic resonance involved in the RE doped crystals and glasses, laser cooling of semiconductors exhibits a number of advantages[7,8]. Semiconductors are anticipated to exhibit more efficient pump light absorption, much lower achievable cooling temperature and direct integrability into electronic and photonic devices. Although many theoretical and experimental studies have addressed various aspects of the laser cooling of semiconductors, no net cooling has been achieved in semiconductors until recently the first demonstration of net laser cooling was achieved in CdS nanobelts by our group[9]. We will elaborate the laser cooling in CdS nanobelts in the following.

2. SETUP AND RESULTS

Figure 1a shows the anti-Stokes luminescence spectra of a CdS nanobelt excited by a 532 and 514 nm laser at 294 K for three different pumping power. Strong anti-Stokes emission with a peak position ~ 506 nm is identified. It should be noted that 514 nm pumping led to much stronger upconversion due to larger bandtail absorption. The strong anti-Stokes luminescence may originate from two-photon absorption or from phonon-assisted transition. The difference can be distinguished through the excitation power dependence of the anti-Stokes luminescence intensity. Systematic study on anti-Stokes luminescence intensity versus laser power (Figure 1b) indicates that two-photon absorption can be excluded under a low-moderate power (~ below 12 mW) for both 532 and 514 nm laser pumping, at which our laser cooling experiments were conducted.

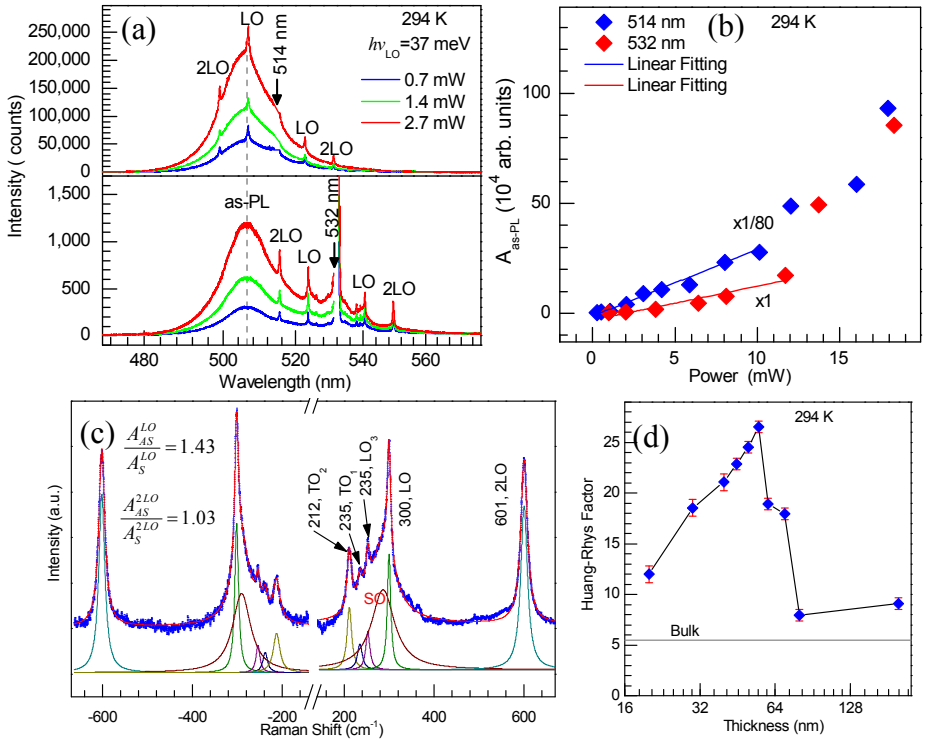

Figure 1 (a) Room temperature anti-Stokes PL spectra of a single CdS nanobelt (100 nm) excited by a 514 nm (top frame) and 532 nm (bottom frame) laser at three power levels. (b) Power dependence of anti-Stokes photoluminescence pumped by 532 and 514 nm at 294 K. The single photon process dominates below ~ 12 mW, above which the two-photon absorption process is significant. (c) Raman lineshape analysis of a single CdS nanobelt excited by a 532 nm laser at room temperature. The PL background has been subtracted. Experimental integral intensity ratios of anti-Stokes and Stokes 1LO and 2LO are

indicated in the plot. (d) Huang-Rhys Factor as a dependence on the nanobelt thickness. The gray line is the value we evaluated for bulk CdS crystal based upon the Raman spectrum data. Adapted from Ref.[9] with permission.

The resonant annihilation of one or more longitudinal optical (LO) phonons facilitates the strong anti-Stokes luminescence owing to the strong coupling between excitons and LO phonons in CdS nanobelts. Figure 1c displays the Raman peak assignments and peaks fittings of a single CdS nanobelt excited by a 2.7 mW 532 nm laser at room temperature. The emission background has been subtracted in order to examine the Raman intensity. All the features can be clearly identified as labeled in Figure 1c. For both 1LO and 2LO phonon scattering, the anti-Stokes components are stronger than their Stokes counterparts. The intensity of the Stokes Raman scattering indicates the creation of the phonons while the intensity of the anti-Stokes Raman scattering reflects the annihilation of the phonons. Stronger anti-Stokes component indicates that the phonon annihilation process dominates over the creation process. Furthermore, Huang-Rhys factor *S*, which is used to quantify the electron-phonon coupling strength, is significantly enhanced in CdS nanobelts suggesting that enhanced electron-phonon coupling in CdS nanobelts (Figure 1d). Therefore, we conclude that the resonant annihilation of one or more LO phonons facilitates anti-Stokes luminescence in CdS nanobelts.

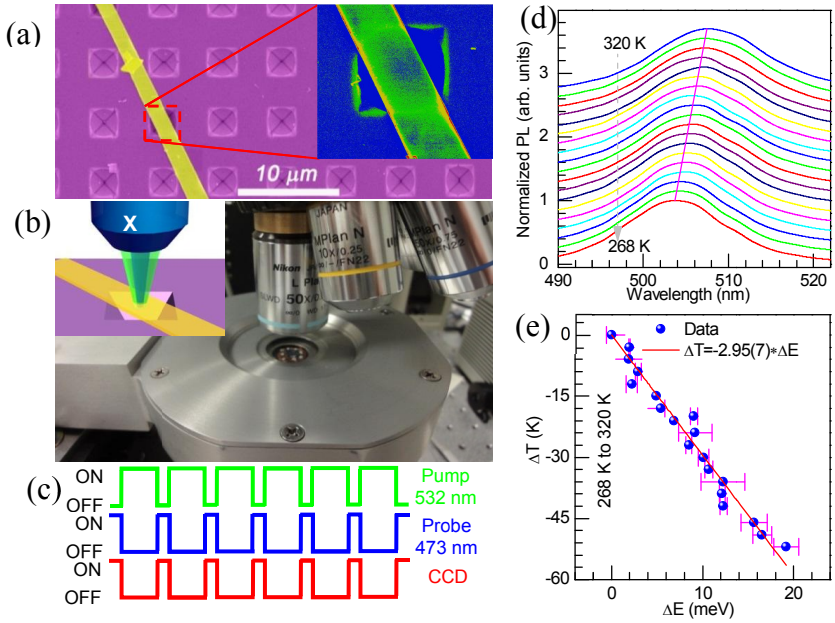

Figure 2 (a) SEM image of a single CdS nanobelt suspended on a SiO_2/Si substrate. Laser cooling demonstration was conducted on the suspended segment as shown in the inset. (b) The measurement set-up with two laser beams (pump and probe) aligned at the same spot. (c) The time sequence of the PPLT. (d) The temperature dependence of the Stokes PL spectra excited by a 473 nm laser from 320 K to 268 K. (e) The temperature differences versus peak shifts in energy, both referenced to 320 K. Adapted from Ref.[9] with permission.

To precisely determine the local temperature variation at the sample upon laser cooling, we adopt a pump-probe luminescence thermometry (PPLT) technology, which is based on the sensitivity of the luminescence peak blue (red) shifts when the temperature is decreased (increased). The band edge emission of semiconductors follows a Varshni equation[10]. Essentially, the PPLT is similar to differential luminescence thermometry[11], except that the cooling effect in semiconductors observed here is so pronounced such that the differential method is not necessary. The sample image, setup and time sequence are schematically shown in Figure 2a, 2b and 2c, respectively. The CdS nanobelt was suspended across holes (~ 3 μm width) on a SiO_2/Si substrate etched by a potassium hydroxide solution. Using such patterned substrate and suspended geometry, the thermal conductive loss through substrates can be minimized and the luminescence escape efficiency can be further improved. The sample was mounted on the cold finger of a continuous flow microscopy cryostat. A solid

state 532 nm laser and Argon ion laser (514 nm, 502 nm and 488 nm) were used as pump lasers, while a 473 nm solid state laser was used as a probe beam measure the Stokes PL in order to deduce the local sample temperature. The probe beam of 473 nm was kept as low as 20 μW. Both pump (Argon ion laser and solid state 532 nm laser) and probe beams were collimated and focused thorough a 50× objective onto a single CdS nanobelt on the suspended segment. The scattered photons were collected by the objective and analyzed by a confocal triple grating spectrometer (Horiba-JY T64000) in a backscattering configuration. The signal was then recorded by a liquid-nitrogen cooled charge-coupled device. The spectrometer has a 640 mm focal length and is equipped with a 1,800/mm grating with a spectral resolution ~ 0.5 cm^{-1}, corresponding to ~ 0.01 nm around 500 nm. During the cooling experiments, each Stokes PL spectrum was recorded after an interval of ~5-min pumping, when the pump laser was blocked momentarily, while the block was removed immediately after the spectrum was collected.

Firstly, the temperature calibration curves was determined by monitoring the Stokes PL peak shift of the CdS nanobelt excited by the probe beam at a given temperature. To calibrate the peak shift versus temperature change, the peak position of the Stokes PL spectra as a function of an accurate sample temperature is demanded. This was achieved by accurately measuring the temperature of a copper cold finger of a continuous flow microscopy cryostat. The silicon substrate was glued onto the cold finger by GE varnish to ensure good thermal contact. The cold finger temperature can be precisely controlled by a temperature controller and accurately measured by a silicon diode temperature sensor, which is enclosed inside a radiation shielding box. Adequate waiting time was ensured to allow the system to reach a thermal equilibrium. Then, these calibration curves are used to deduce the laser cooling temperature.

The calibration spectra and calibration curve for a 100 nm thick CdS nanobelt are given in Figure 2d and 2e, starting from 320 K. Calibration curve in Figure 2e is extracted from Figure 2d, plotted as temperature changes (referenced to the starting temperature 320 K) versus the PL peak shift in energy (meV). The calibration curve can be fitted linearly. This is a good approximation of the Varshni equation when the temperature range is small.

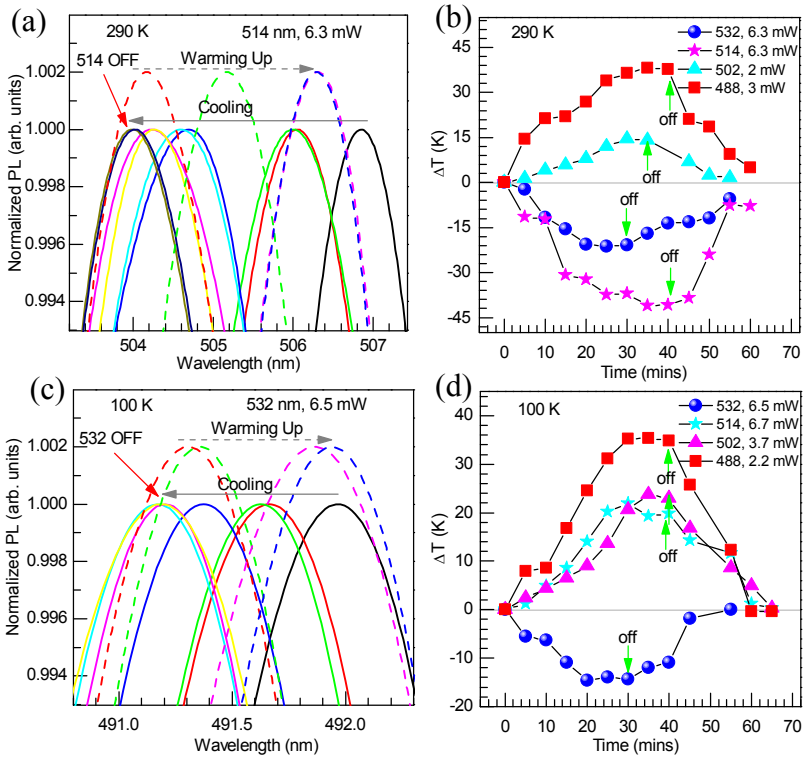

Figure 3 (a) The evolution of PPLT spectra starting from 290 K, pumped by 514 nm with a power of ~ 6.3 mW. Solid curves represent the cooling cycle, while the dashed curves represent the warming up after the pump laser is switched off. Dashed curves are shifted vertically for clarity. (b) The temperature change ΔT versus time pumped by four laser lines (532, 514, 502 and 488 nm). (c) The evolution of PPLT spectra for another nanobelt pumped by 532 nm laser with 6.5 mW starting from 100 K. Similar cooling and warming up cycles are observed as shown in (a). (d) The Temperature change ΔT versus time pumped by four laser lines (532, 514, 502 and 488 nm). Adapted from Ref.[9] with permission.

For clarity, we only show the data with a continuous 6.3 mW 514 nm and 6.5 mW 532 nm laser pumping, starting from 290 K and 100 K, respectively. Solid curves represent the cooling cycle, while the dashed curves represent the warming up after the pump laser is switched off. Dashed curves are shifted vertically for clarity. A pronounced systematic blue shift is observed upon laser pumping until a steady state is reached in ~30-40 minutes, suggesting that a maximum net cooling is established. After the cooling is stopped (switching off pump laser), the Stokes PL red shifts, indicating a temperature rise. Based on the calibration curves shown in Figure 2e, the temperature change ΔT extracted from Figure 3a and 3c is plotted in Figure 3b and 3d, which show a net laser cooling of ~40 K and 20 K for 514 and 532 nm pumping at 290 K, respectively. At 100 K, only 532 nm can lead to a net laser cooling of ~15 K while 514 nm laser cannot due to red shifting of the mean emission wavelength at 100 K. 488 and 502 nm laser pumping leads to heating of the sample at all temperatures.

According to Sheik Bahae-Epstein (SB-E) theory[7,12], the cooling efficiency $\eta_c(\hbar v,\ T)$ of optical refrigeration in semiconductors follows:

$$\eta_c(\hbar v,\ T) = \eta_{exe}\eta_{abs}\frac{\overline{v}_f(T)}{v} - 1\,, \tag{1}$$

where v is the pump laser frequency, T is the temperature of the sample, and $\overline{v}_f(T)$ is the escaped mean emission frequency evaluated by normalizing the intensity at different wavelength. η_{exe} is the external quantum efficiency being written as $\eta_{exe} = \eta_e W_{rad}/(\eta_e W_{rad} + W_{nr})$, where η_e is the luminescence extraction efficiency, W_{rad} and W_{nr} are the radiative and non-radiative recombination rates, respectively. $\eta_{abs} = [1+\alpha_b/\alpha(v,T)]^{-1}$ is the absorption efficiency, quantifying the percentage of photons absorbed that are engaged in cooling, where α_b is the background absorption coefficient and $\alpha(v,T)$ is the semiconductor absorption coefficient.

The pump lasers (*e.g.*, 514 or 532 nm) move to the Urbach tail of CdS, nevertheless the photoconductivity and PL measurement suggest that the background absorption due to free carriers or surface contribution in a CdS nanobelt is negligible[9]. The luminescence extraction efficiency approaches unity because of sub-wavelength thickness. Compared to GaAs, CdS has a much smaller surface recombination speed[13] and much lower Auger non-radiative recombination coefficient[14]. Our previous data[15] and more in-depth analysis have indeed revealed that the radiative recombination decay lifetime is on the order of tens to hundreds of picoseconds, while the non-radiative decay lifetime is three orders of magnitude larger at room temperature and even more at low temperatures, justifying the nearly unity external quantum efficiency of >99% in CdS nanobelts[9]. Applying the equation (1), a cooling efficiency of ~4.8% at 290 K and ~2.0% for 100 K are estimated for 532 nm pumping, while a cooling efficiency of 1.3% for 514 nm pumping at 290 K.

Starting from equation (1), the cooling power can be defined as:

$$P_{cool} = \eta_c\alpha(v,T)tP_0 = \frac{\alpha(v,T)tP_0\left[\eta_{exe}\eta_{abs}h\overline{v}_f(T) - hv\right]}{hv} \tag{2}$$

Considering the nanobelt used with a thickness of 100 nm, we have obtained a high external quantum efficiency ($\eta_{exe} \approx 99.5\%$) and zero background absorption ($\alpha_b = 0$, thus $\eta_{abs}(v,T) = \alpha(v,T)/[\alpha(v,T)+\alpha_b] = 1$) for the suspended sample configuration. Therefore, by taking $\eta_{exe} \approx 1$ and $\eta_{abs}(v,T) = 1$, the equation (2) can be re-written as:

$$P_{cool} = \alpha(v,T)tP_0\Delta E/hv \tag{3}$$

where P_0 is the power of the incident laser, t is the thickness of the nanobelt and energy blue shifting parameter $\Delta E = h\bar{\nu}_f(T) - h\nu$. Based on $\alpha(532\ nm) = 3\times10^4\ cm^{-1}$, and 100 nm thickness of nanobelt, we obtained the cooling power $P_{cool} \approx 97\ \mu$W for -20 K cooling pumped by 6.3 mW 532 nm laser starting from 290 K. For 514 nm pumping, the $\alpha(514\ nm) = 1.8\times10^5\ cm^{-1}$, the corresponding cooling power is ~197 μW for -40 K cooling. From the above analysis, it is important to note that high cooling efficiency does not necessarily lead to high cooling power, as the final cooling power depends on both energy blue shifting parameter and bandtail absorption.

For our experimental setup, the thermal dissipation consists of two possible contributions: the first one is the radiative load, and the other one is the thermal conductive contribution from the substrate heat sink. Based on the theory of the black body radiation, the radiative load can be negligible. For the thermal conductive load, the conductive loss power can be expressed as follows:

$$P_{cond} = k(T_c - T_s)\cdot S/\Delta L, \tag{4}$$

where k is the thermal conductivity of CdS ($k = 20\ \mathrm{W\cdot m^{-1}K^{-1}}$)[16], ΔT is the temperature difference between local cooling point and heat sink of substrate, S (~0.2 μm^2) is the cross-section area of CdS nanobelt and ΔL (~1 μm) is the length between laser spot to the edge of SiO_2 hole. Therefore, we estimated $P_{cond} = 80\ \mu$W for -20K cooling pumped by 6.3 mW 532 nm laser starting from 290 K. This value is very close to the calculated cooling power $P_{cool} \approx 97\ \mu$W.

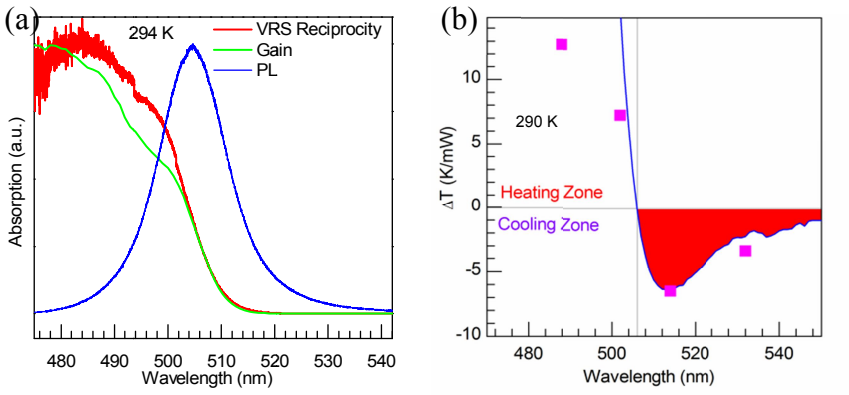

Figure 4 (a) The phtoconductivity gain (green) and calculated absorption spectra from the PL spectrum (blue) by van Roosbroeck-Shockley relation (red). (b) Summary of measured maximum ΔT (pink square) and theoretically calculated temperature change curve (solid blue) normalized to pump power in K/mW for different pump wavelengths at 290 K. The red region corresponds to the cooling zone. Adapted from Ref.[9] with permission.

At the single nanobelt level, the direct measurement of optical absorption remains elusive. We devise a photoconductivity measurement to provide a direct quantification of the absorption[17], which agrees well with the absorption coefficient extracted from the PL spectra based upon the van Roosbroeck-Shockley equation, as shown in Figure 4. At room temperature and under a small applied source-drain voltage, the gain of the photoconductivity $G(v)$ is proportional to the absorption coefficient, $\alpha(v)t = KG(v)$, where $K = 0.15$ for t=100

nm nanobelt. By using photoconductivity spectroscopy, we obtain $G(v)$ for an individual nanobelt at 290 K. Therefore, the *normalized temperature change* $\Delta T/P_0$ can be written as:

$$\frac{\Delta T}{P_0} \equiv \frac{T_S - T_C}{P_0} = -\frac{\varsigma K \Delta L}{kShv} G(v, T_C)\Delta E \equiv \frac{-\chi \cdot G(v, T_C)\Delta E}{hv}, \quad (5)$$

where $\chi = \frac{\varsigma K \Delta L}{kS}$ and ς is the correction parameter. For the different pump energies and low excitation powers, the mean emission wavelength of the luminescence is approximately equal to a constant. For ~100 nm CdS nanoblets, the mean wavelength of the luminescence is ~506 nm at 290 K. For a 532 nm laser with a power of 6.3 mW, $\Delta T = -20$ K which gives $\varsigma = 0.82$ and $\chi = 30.8\ \mathrm{K \cdot mW^{-1}}$. Applying the obtained χ to equation (5), the calculated *normalized temperature change* can be obtained. It is important to note that the excitonic effect was not discussed in detail here, because in CdS the excitons are usually completely ionized due to strong exciton phonon coupling. As a result, the photo-generated electron-hole bound states dissociate at room temperature and contribute to the photocurrent. Therefore, it is accurate to use photoconductivity gain to quantify the absorption.

Figure 4a displays the Stokes PL (black curve), the corresponding photoconductivity gain spectra (blue curve) and absorption coefficient extracted from the PL spectra based upon the van Roosbroeck-Shockley equation at 290 K. We find that at 532 nm, there is about 6% absorption compared to the maximum absorption around 480 nm, while at 514 nm, this value is ~ 24%. Based on expression (5), Figure 4b shows the normalized temperature change as a dependence on pumping laser wavelength at 290 K (blue curve). The pink squares are the measured cooling temperature change normalized to pump laser power under different excitation wavelengths. Here, $\Delta T/P_0$ <0 corresponds to the cooling zone and $\Delta T/P_0$ >0 indicates the heating zone. When the pump laser energy is equal to the mean energy of luminescence, the heating and cooling cancel each other and result in with a vanishing $\Delta T/P_0$. The experimental temperature change ΔT in K/mW pumped by four different laser lines is in good agreement with theoretical analysis except for 488 nm. The final cooling power depends on both ΔE and bandtail absorption. In CdS nanobelts at 290 K, 514 nm appears as the optimal cooling wavelength with the highest cooling power. The red region corresponds to the laser cooling tail.

In summary, we have presented the concrete evidence of laser cooling a semiconductor using a semiconductor CdS nanobelt. We have achieved ~40 K cooling from room temperature pumped by 514 nm, while ~15 K from 100 K pumped by 532 nm. The cooling efficiency is estimated to be ~4.8% at 290 K and ~2.0% at 100 K for 532 nm pumping, while a cooling efficiency of 1.3% for 514 nm pumping at 290 K. The cooling power is estimated to be ~ 97 and 180 μW for 532 nm and 514 nm pumping at 290 K, respectively. The thermal conductive load of our device is estimated to be about 80 and 160 μW, in good agreement with the cooling power, since the radiative load is negligible based on a black body model for both wavelengths. The achievement of the net laser cooling in CdS nanobelts can be attributed to the strong coupling between electron and longitudinal optical phonons, high external quantum efficiency and negligible background absorption. Our work suggests the considerable potentials of II-VI semicondcutors for optical refrigeration. It would be an immediate attempt to see whether laser cooling can be achieved below liquid nitrogen temperature, in which rare-earth doped system loses the cooling power due to Boltzmann's distribution of carriers.

ACKNOWLEDGMENTS

We thank M. Sheik-Bahae and R. Merlin for helpful discussions. Q.X. acknowledges the support from the Singapore National Research Foundation through a fellowship grant (NRF-RF2009-06). This work was also supported in part by the Singapore Ministry of Education via a Tier 2 grant (MOE2011-T2-2-051) and start-up grant support (M58113004) from Nanyang Technological University.

REFERENCES

1 Pringsheim, P. "Zwei Bemerkungen über den Unterschied von Lumineszenz- und Temperaturstrahlung". *Zeitschrift für Physik A Hadrons and Nuclei* **57**, 739-746, (1929).

2 Vogl, U. & Weitz, M. "Laser cooling by collisional redistribution of radiation". *Nature* **461**, 70-73, (2009).
3 Kastler, A. "Quelques suggestions concernant la production optique et la détection optique d'une inégalité de population des niveaux de quantifigation spatiale des atomes. Application à l'expérience de Stern et Gerlach et à la résonance magnétique". *J. Phys. Radium* **11**, 255-265, (1950).
4 Epstein, R. I. *et al.* "OBSERVATION OF LASER-INDUCED FLUORESCENT COOLING OF A SOLID". *Nature* **377**, 500-503, (1995).
5 Sheik-Bahae, M. & Epstein, R. I. "Optical refrigeration". *Nature Photonics* **1**, 693-699, (2007).
6 Seletskiy, D. V. *et al.* "Local laser cooling of Yb:YLF to 110 K". *Opt. Express* **19**, 18229-18236, (2011).
7 Sheik-Bahae, M. & Epstein, R. I. "Can laser light cool semiconductors?". *Physical Review Letters* **92**, (2004).
8 Rupper, G., Kwong, N. H. & Binder, R. "Large excitonic enhancement of optical refrigeration in semiconductors". *Physical Review Letters* **97**, (2006).
9 Zhang, J., Li, D., Chen, R. & Xiong, Q. "Laser cooling of a semiconductor by 40 Kelvin". *Nature* **493**, 504, (2013).
10 Li, D., Zhang, J. & Xiong, Q. "Surface Depletion Induced Quantum Confinement in CdS Nanobelts". *ACS Nano* **6**, 5283-5290, (2012).
11 Imangholi, B. *et al.* (eds Marek, O., Fritz, H., & Yasuhiko, A.) 61151C (SPIE).
12 Sheik-Bahae, M. & Epstein, R. I. "Laser cooling of solids". *Laser & Photonics Reviews* **3**, 67-84, (2009).
13 Huppert, D., Evenor, M. & Shapira, Y. "Summary Abstract: Measurements of surface recombination velocity on CdS surfaces and Au interfaces". *Journal of Vacuum Science & Technology A: Vacuum, Surfaces, and Films* **2**, 532-533, (1984).
14 Imangholi, B. "Investigation of laser cooling in semiconductors" Ph.D. thesis, The University of New Mexico, (2006).
15 Xu, X. *et al.* "Dynamics of bound exciton complexes in CdS nanobelts". *ACS Nano.* **5**, 3660-3669, (2011).
16 Madelung, O., Rössler, U. & Schulz, M. [Landolt-Bornstein, Group III: Condensed Matter. Semiconductors: II-VI and I-VII compounds, Vol. 41B]. Springer, Berlin Heidelberg (1999).
17 Li, D. H., Zhang, J., Zhang, Q. & Xiong, Q. H. "Electric Field-Dependent Photoconductivity in CdS Nanowires and Nanobelts: Exciton ionization, Franz-Keldysh and Stark Effects.". *Nano Lett.* **12**, 2993, (2012).